Geosci. Model Dev. Discuss., 6, 1127–1172, 2013
www.geosci-model-dev-discuss.net/6/1127/2013/
doi:10.5194/gmdd-6-1127-2013


Geoscientific Model Development Discussions
Open Access







# The GREENROOF module (v7.3) for modelling green roof hydrological and energetic performances within TEB

**C. S. de Munck[1], A. Lemonsu[1], R. Bouzouidja[2,3], V. Masson[1], and R. Claverie[3]**

[1]Météo France, CNRS-GAME, UMR3589, Centre National de Recherches Météorologiques, Toulouse, France
[2]NIDAPLAST, Thiant, France
[3]Centre d'Études Techniques de l'Équipement de l'Est, Tomblaine, France

Received: 21 December 2012 – Accepted: 4 February 2013 – Published: 20 February 2013

Correspondence to: C. S. de Munck (cecile.demunck@meteo.fr)

Published by Copernicus Publications on behalf of the European Geosciences Union.

## Abstract

The need to prepare cities for climate change adaptation requests the urban modeller community to implement within their models sustainable adaptation strategies to be tested against specific city morphologies and scenarios. Greening city roofs is part of these strategies. In this context, a GREENROOF module for TEB (Town Energy Balance) has been developed to model the interactions between buildings and green roof systems at the scale of the city. This module allows one to describe an extensive green roof composed of four functional layers (vegetation – grasses or sedums, substrate, retention/drainage layers and artificial roof layers) and to model vegetation-atmosphere fluxes of heat, water and momentum, as well as the hydrological and thermal fluxes throughout the substrate and the drainage layers, and the thermal coupling with the structural building envelope. TEB-GREENROOF (v7.3) is therefore able to represent the impact of climate forcings on the functioning of the green roof vegetation and, conversely, the influence of the green roof on the local climate. A calibration exercise to adjust the model to the peculiar hydrological characteristics of the substrates and drainage layers commonly found on green roofs is performed for a case study located in Nancy (France) which consists of an extensive green roof with sedums. Model results for the optimum hydrological calibration show a good dynamics for the substrate water content which is nevertheless under-estimated but without impacting too much the green roof temperatures since they present a good agreement with observations. These results are encouraging with regard to modelling the impact of green roofs on thermal indoor comfort and energy consumption at the scale of cities, for which GREENROOF will be running with the building energy version of TEB, TEB-BEM. Moreover, the green roof studied for GREENROOF evaluation being a city-widespread type of extensive green roof, the hydrological characteristics derived through the evaluation exercise will be used as the standard configuration to model extensive green roofs at the scale of cities.

## 1 Introduction

In the literature, green roofs (roofs with a vegetated surface and a growing media) have been credited with a large number of environmental benefits. Many experiments conducted on green roofs have highlighted their potential to reduce roof run-off entering the storm water systems through retention and evapotranspiration. This has been demonstrated at the site scale (Berghage et al., 2009; Voyde et al., 2010 are two good examples), and at the city (Mentens et al., 2006) and landscape (Oberndorfer et al., 2007) scales. Reduced roof run-off also implies reduced rain water pollutants entering storm water systems (Berndtsson et al., 2009) although this benefit may slightly be counter-balanced by the additional source of pollution represented by the green roof substrates themselves (Oberndorfer et al., 2007). Considering energy aspects, green roofs have the ability to moderate temperature changes within buildings (Castleton et al., 2010), with beneficial consequences on building energy consumption (Getter and Rowe, 2006; Castleton et al., 2010; Jacquet, 2011) due to increased roof solar reflectivity, increased thermal mass, shading and evaporative cooling (compared to standard roofs). As for energy savings, it may vary with the season and the green roof design (materials and thicknesses) although it seems strongly influenced by the level of insulation of the structural roof (Jaffal et al., 2012). Jacquet (2011) observed for a green roof plot in Montréal a reduction in air conditioning demand in summer of 98.9 and 90.8 % (respectively when the green roof was irrigated and not) and a milder reduction in heating demand in winter (38.3 and 27.4 % depending on irrigation again). All these site-based evidences for green roof benefits have now contributed to promote the use of city-scale green roof infrastructure as a sustainable adaptation strategy for climate change (Bass and Baskaran, 2003; EEA, 2012; Foster et al. 2011; Giguère, 2009; Lawlor et al., 2006; Penney, 2008; USEPA, 2008). The implementation of green roofs compared to urban forests and street trees, may represent a more realistic and efficient greening strategy at the heart of cities where the building fraction is high (and the ground-base surface available for greening scarce) and the initial evapotranspiration potential low.

The need for taking this research from the building scale to that of the city is clear, especially in the light of climate change. A modelling approach is the only realistic way an adaptation strategy such as roof greening can be evaluated city-wide and for various seasons or long time series, hence the need for green roof models. So far, very few studies have attempted to quantify the potential of green roof infrastructures at city-scale. Three studies were found but which do not represent green roofs (nor buildings) explicitly. In these studies, building roofs are replaced by natural evaporating surfaces (grass, ground level) and energy and hydrological transfers are simulated with very simple parameterizations and calibrations. Bass et al. (2003) attempted to quantify the potential of green roofs for urban heat island (UHI) mitigation using this kind of modelling approach. They simulated the greening of 50 % of the available roof surfaces throughout the city of Toronto (by replacing roof surfaces with grass) and predicted a mild cooling over part of the city on the order of 0.5 °C without irrigation, and a greater and spatially wider cooling (2 °C) with irrigation of the "green roofs" and the ground-level grass of the densest areas of Toronto. Gill et al. (2007) compared the impact of green roofs on surface temperatures (based on a simple energy balance equation) and run-off (via a standard runoff curve number approach) for various urban morphology classes (UMC) for the conurbation of Greater Manchester in the UK. They showed that "greening" all roofs made the most significant contribution to maximum surface temperature and runoff reduction in the most urbanised UMCs (respectively 6.6 °C and 17.6 % for the town centre). Following Bass et al., (2003) approach, Rosenzweig et al. (2009) suggested that a "green roof" infrastructure for New York City could reduce urban air temperatures by 1.4 °C on average and 3.2 °C at best, which should lead to a reduction in UHI amplitude. More detailed models are needed for city-scale applications that can explicitly describe green roofs and the thermal and hydrological behaviours associated with them, so that their impacts in terms of building energetics, comfort, UHI and runoff be more accurately evaluated. With this aim, a detailed green





GMDD
6, 1127–1172, 2013

roof model should be integrated in an urban canopy model in order to be run under imposed (present or future) climatic conditions or coupled to a meteorological model. This way, the environmental benefits highlighted at the building-scale could be studied and quantified more widely, more accurately and under various climatic constraints.

In order to set up a strategy for implementing green roofs within our Town Energy Balance (TEB) urban canopy model (Masson, 2000; Hamdi and Masson, 2008), a review of the types of green roof implemented in cities nowadays was primarily undertaken (Sect. 2). This allowed us to determine the main design and functions that a green roof model should describe and consequently the physical processes associated that need to be captured. There followed a review of green roof modelling studies to establish an inventory of existing green roof models, both with regard to their complexity and their research objectives. On these bases, a green roof parameterization has been developed for TEB. The implementation of this GREENROOF module was part of a wider effort to implement various types of urban vegetation within the model TEB (Lemonsu et al., 2012). The hypothesis and the parameterization of GREENROOF are presented (Sect. 3), followed by a calibration exercise for an extensive green roof plot in the North East of France (Sect. 4). This exercise, focused on the hydrological properties of the green roof allowed to identify a set of values for these properties that best fitted with in-situ conditions. The results are presented both with regard to the hydrological performance of the green roof and its thermal performance.

## 2 Strategy for modelling green roofs within TEB

### 2.1 Generic design of a green roof and physical processes associated

Green roofs of two types can be found in cities. Those called “rooftop gardens” support fairly large shrubs or trees. Due to the intensive care needed at implantation and management, they are commonly called “intensive green roofs” and are generally implemented for recreational use. Those containing only one or two low-profile plant species and therefore requiring a minimal growing media, are called “extensive”. They are often used for improved thermal and hydrological performances (Wark and Wark, 2003) and are thus interesting to model as adaptation strategy.

Based on the technical and scientific literature (Wark and Wark, 2003; Lazzarin et al., 2005), a generic design for extensive green roofs can be reached. From top to bottom, the essential components are a layer of vegetation, a layer of soil-forming-material called substrate which is the growing media for the vegetation, a different soil-forming-material layer which helps to control the moisture status of the over-laying substrate (drainage or retention function depending on the plant species/climate association) and a mandatory waterproofing sheet to prevent the structural roof from water damages. Therefore, the final green roof design can be considered as the superposition of a “natural” compartment (vegetation and different soil-forming-material layers) and of an artificial compartment (waterproof and structural roof materials).

In addition, experimental studies on pilot green roofs (for example Bass and Baskaran, 2003; Berghage et al., 2009, Jacquet, 2011; Jim and He, 2010; Jim, 2011, Jim and Peng, 2011; Nardini et al., 2012) have highlighted within these “natural” layers heat and water transfers which are similar to those which establish themselves within ground-level natural surfaces, except for specific limit conditions. The transfers involved in a natural surface, be it at ground or roof-level, are energetic, thermal and hydrological. The energy balance results in the balance between the surface net radiation and the latent, sensible and storage heat fluxes. Heat conduction and storage occur and can be strongly influenced by soil moisture status. But unlike open ground natural surfaces, for green roof natural surfaces the heat gains or losses from the thermal contact with the bearing roof should be considered. In terms of hydrological transfers, a green roof surface behaves like any other natural surface (vertical water fluxes depend on soil moisture gradients, drainage appears if super-saturated conditions appear and run-off may establish in response to extreme rainfall events) except that the hydrological characteristics of green roof soil-forming-materials are very different from those of natural soils and that the water drained out of green roof base is lost “in favour of” the rainwater





GMDD
6, 1127–1172, 2013

network. These differences do not change the nature of the transfers involved but act rather as limit conditions for these transfers.

Therefore, it seems realistic to make the hypothesis that the natural layers of green roofs could be simulated by a standard soil-vegetation model incorporating the limit conditions presented hereby associated with the finite dimension of the green roof and the presence of a structural built roof at its base.

## 2.2 State-of-the-art in green roof modelling

A state of the art of green roof models highlights two modelling topics: that of the energy performance, and that of the hydrological performance, the two rarely combined. The simple thermal and hydrological approaches are not presented here because they do not meet the criteria defined in our objectives.

All the detailed models of heat transfer (Alexandri and Jones, 2007; Del Barrio, 1998; Kumar and Kaushik, 2005; Ould-Boukhitine et al., 2011; Sailor, 2008 – also known as the *Ecoroof* module for *EnergyPlus*) have in common an explicit description of green roofs, which takes into account a structural roof model, a soil model and a canopy model. While the energy balance at the green roof surface is performed in a more or less complex way (especially with regard to modelling the behaviour of the vegetation), the heat transfer is subsequently simulated by all these models based on a standard conduction equation. As far as modelling vegetation behaviour is concerned, all models propose to parameterize vegetation transpiration as a function of the meteorological conditions and the gaseous equilibrium which establishes between the outside and the inside of the plant (via the plant stomatal resistance) except that of Ould-Boukhitine et al. (2011) which uses a simpler formulation (Penman-Monteith). Although these models account for the hydrological status of the green roof, it is with the sole purpose of computing soil effective thermal characteristics (as in function of soil moisture). Soil moisture status is either measured or estimated via a simple or a mixed form of Richard's equation, but hydrological performance is generally not evaluated.

Most of the studies aimed at modelling the hydrology of green roofs (Hilten et al., 2008; Palla et al., 2009, 2012) used the HYDRUS software (Simunek et al., 1994, 2005). This calibrated model relies on the Richard's equation and on the hydraulic functions of Van Genuchten (1980) and Mualem (1976) to simulate the processes of infiltration, lateral flow and surface runoff and predict moisture content profiles. Although very detailed, this model needs user-input evapotranspiration rates, which must therefore be estimated by other means. For numerical reasons, HYDRUS works at very fine spatial resolutions, so that it is used to evaluate the hydrological performance of a green roof at the scale of the hydrological event (generally a few hours). Although it now takes into account the heat transport in addition to detailed hydrological processes (Simunek et al., 2005; Yu and Zheng, 2010), it is consequently not adapted for the city-scale applications.

In summary, even if most models are able to capture the dominant processes involved in green roof soil and structural compartments, none of them currently couple a combined modelling of thermal and hydrological processes that could be used on the scale of a city. Neither is the presence and impact of drainage or retention layers simulated, while they play a major role, not only with regard to hydrological performance but also in terms of thermal performance, as evidenced by the work of Jim and Tsang (2011). Finally, the difficulty encountered by all models remains the calibration, as is the case for all models with these levels of complexity.

## 2.3 Strategy for the inclusion of green roofs within TEB

As we have established that the heat and water transfers involved in the natural layers of green roofs (atmosphere, vegetation, and substrate and hydrological control layers) are similar to those of perfectly natural surfaces, they can therefore be simulated, as is the case in the models previously examined, by a standard soil and vegetation model, provided that it is calibrated to reflect the peculiar characteristics of the soil-forming-materials used for the construction of green roofs. Therefore, the strategy that we propose and ultimately retain for the inclusion of green roofs within TEB is to use a soil and vegetation model that can, not only be calibrated for a specific soil, but would also have the ability to overcome the limitations of existing models. The ideal model should allow for a coupled modelling of green roof hydrological and energetic performances, dispose of sufficiently detailed parameterizations to describe the physical processes involved (including evapotranspiration and soil water flows), and at the same time have spatial resolutions (i.e. time calculations) suitable for our modelling objectives at city-scale.

## 3 A green roof module for TEB

### 3.1 Current modelling of the urban climate with TEB

Urban climate modelling at the CNRM-GAME Research Centre relies on the use of the SURFEX land surface modelling system (Masson et al., 2012). It characterizes a study area based on four land use types (urban, natural, freshwater and sea and ocean surfaces) and computes the exchange of heat, water, momentum between each type of surface and the atmosphere. More especially, SURFEX features TEB (Masson, 2000) for solely urban surfaces and the ISBA model (Interaction between Soil Biosphere and Atmosphere) developed by Noilhan and Planton (1989) for the natural and agricultural surfaces.

For TEB, the urban landscape is simplified as a network of street canyons of infinite length. Within each surface resolved by the model (also called mesh), it is possible to specify the geometric, radiative and thermal characteristics of an average street canyon represented (for equiprobable street orientations) or to fix these features street canyon by street canyon (for different street directions). TEB simulates the exchange of heat and water for three generic surfaces (roof, wall and road) and computes the urban microclimate variables at street level, as well as energy and water budgets from the neighbourhood to the city scale (Lemonsu et al., 2004, 2010; Offerle et al., 2005; Pigeon et al., 2008) and the feedback on the meteorological variables when it is coupled to an atmospheric model (de Munck et al., 2013; Lemonsu and Masson, 2002).

Recently, to better describe the finer scale interactions between artificial surfaces and natural surfaces found within cities, the ISBA model used for natural and agricultural surfaces has been integrated within TEB (resulting in the TEB-Veg configuration) and evaluated by Lemonsu et al. (2012). Given the modelling strategy retained and the willingness to optimize source code development while retaining the modular structure of the SURFEX tool, an approach similar to Lemonsu et al. (2012), relying on ISBA, was considered well adapted and detailed enough to characterize and simulate water, energy and momentum fluxes within the natural layers of green roofs.

### 3.2 Using ISBA-DF coupled with TEB for modelling green roofs

Given the different roles and behaviours of the "soil" compartments of a green roof (substrate and drainage/retention layers) and the vertical "soil" texture heterogeneity associated, it is the diffusive version of the ISBA model that is retained (called ISBA-DF for explicit vertical diffusion and developed by Boone et al., 2000) for the modelling of the green roof natural layers. Indeed, because it allows us to represent the vertical heterogeneity of soil (and root profile distribution) and a detailed modelling of hydrological transfers, ISBA-DF has the potential to accurately simulate different hydrological behaviours for a substrate and drainage/retention layers, which appears to be an improvement compared to existing green roof models. Consequently, the green roof design retained for GREENROOF allows four distinct compartments or layers to be modelled (Fig. 1): from top to bottom, a compartment for vegetation which interacts with the atmosphere, a layer of substrate (in which lies the root system of the vegetation), a layer that controls the hydrological exchange with the substrate above (retention/drainage layer), and a compartment to represent the structural building and any artificial roof layers installed (waterproofing or thermal insulation membranes and layers of the bearing roof).

Modelling this physical design within GREENROOF implies a configuration with two models: ISBA-DF to simulate the exchange of heat and water in the natural layers of the roof and TEB to simulate heat exchange within the artificial layers of the roof which have no biological role and within which no transfer of water is involved. The structure of the resulting source code is presented Fig. 2. With ISBA-DF, the transfer of heat and water between the atmosphere, the vegetation, and the soil compartments of the green roofs is simulated through fluxes (Fig. 1) which are connected to each other through the latent heat flux ($LE$) which is the sum of the plant transpiration ($LE_{\mathrm{TR}}$), the soil evaporation ($LE_{\mathrm{G}}$), and the evaporation of the water intercepted by plant foliage ($LE_{\mathrm{V}}$). These fluxes are estimated through detailed parameterizations, especially plant transpiration ($LE_{\mathrm{TR}}$) which integrates the impact of soil water stress and meteorological conditions in the physiological functioning of the plant (stomatal conductance). This constitutes a good level of detail considering the spatial scale aimed at, and participates to accurately simulate the energy balance at the surface of the green roof and consequently the heat conduction ($G$) into the substrate and the layers beyond, which is essential to ensure a good prediction of heat transfers within the green roof system. On the hydrological side, the model is capable of predicting green roof surface runoff that may appear in response to extreme rainfall events. Inside the substrate and the hydrological control layers, ISBA simulates the water fluxes due to vertical moisture gradients ($F$) and the water vertical drainage ($K$) that establishes when these layers exceed supersaturation. This way, the overall water discharge from the green roof (which is frequently recorded) can be estimated by combining the contributions of the total drainage out of the green roof base ($K_{\mathrm{total}}$) and the surface run-off.

In ISBA-DF, the soil hydrology is based on a mixed form of the Richards equation to describe the transfer of water through the soil through Darcy's law (changes in moisture and water potential) when transfers of heat (conduction) are described by a classical Fourier's law. The coupling between heat and water transfers is finally realised through effective soil thermal characteristics which evolve in time with the soil moisture status. The effective thermal capacity of the soil is calculated as the weighting of the heat capacity of water and the heat capacity of the dry soil matrix following Peters-Lidard et al. (1998). Similarly, the effective thermal conductivity of the soil is estimated according to Farouki (1986) as a function of the water content, the soil porosity and the conductivity of the dry soil. This corresponds to the level of details encountered in the most detailed green roof models (Alexandri and Jones, 2007; Del Barrio, 1998; Sailor, 2008). In ISBA-DF, all the soil intrinsic characteristics are estimated based on a set of pedotransfer functions and prognostic equations described in Boone et al. (2000) and Decharme et al. (2011).

Finally, the two-models configuration chosen required to implement a thermal coupling between the base of the hydrological control layer (managed by ISBA-DF) and the artificial layers of the roof (managed by TEB). It is expressed through the heat conduction flux ($G_{\mathrm{N-R}}$) that establishes between the deepest sub layer (referred to as layer $n$) of the natural green roof and the top sub layer (layer 1) of the artificial roof with which the natural roof is in contact:

$$G_{\mathrm{N-R}} = \overline{\lambda}_{\mathrm{N-R}} \left( T_{\mathrm{N}_n} - T_{\mathrm{R}_1} \right) \tag{1}$$

$T_{\mathrm{N}_n}$ and $T_{\mathrm{R}_1}$ are, respectively the temperatures of the deepest sub layer of the natural roof and the top layer of the artificial roof. $\overline{\lambda}_{\mathrm{N-R}}$ is the interfacial thermal conductivity between the two layers, approximated by:

$$\overline{\lambda}_{\mathrm{N-R}} = \frac{2\lambda_{\mathrm{N}_n}}{\Delta z_{\mathrm{N}_n}} \tag{2}$$

with $\lambda_{\mathrm{N}_n}$ the effective thermal conductivity of the bottom layer of the natural roof and $\Delta z_{\mathrm{N}_n}$ its thickness. This modifies the equation predicting the temperature evolution of the top layer of the structural roof (Eq. 1a of Masson, 2000):

$$C_{\mathrm{R}_1} \frac{\partial T_{\mathrm{R}_1}}{\partial t} = \frac{(1 - f_{GR})}{d_{\mathrm{R}_1}} \left( Q^*_{\mathrm{R}_1} - H_{\mathrm{R}_1} - LE_{\mathrm{R}_1} - G_{\mathrm{R}_1-\mathrm{R}_2} \right) + \frac{f_{GR}}{d_{\mathrm{R}_1}} \left( G_{\mathrm{N-R}} - G_{\mathrm{R}_1-\mathrm{R}_2} \right) \tag{3}$$

where $C_{\mathrm{R}_1}$ is the thermal capacity of the artificial layer in contact with the natural roof, $f_{\mathrm{GR}}$ the fraction of roof vegetated, and $Q^*_{\mathrm{R}_1}$, $H_{\mathrm{R}_1}$, $LE_{\mathrm{R}_1}$, $G_{\mathrm{R}_1-\mathrm{R}_2}$ the terms of the surface





GMDD
6, 1127–1172, 2013
The GREENROOF module (v7.3) for TEB
C. S. de Munck et al.

energy balance for the fraction of roof not vegetated. Also, to ensure the continuity in temperature, the temperature of the deepest layer of the green roof is recalled to that of the top artificial layer of the structural building at each time step.

Due to the presence of waterproofing membranes, no hydrological coupling is required between the soil-vegetation model and the building model, and the excess water and the water percolated leave the system and are collated as the "green roof outlet drainage". This will allow for connection to urban drainage systems when these will be developed within a future version of TEB.

### 3.3 GREENROOF input parameters

For a given green roof design, the three "natural" compartments implemented in the GREENROOF module (vegetation, substrate and hydrological control layers) can be initialized (Table 1). The study of the scientific and technical literature shows that the plant species the most commonly used on green roofs are grasses (*Gramineae*) or sedums (*Sedum*) or a mixture of both. However, sedums are more frequently used for green roofs implemented under a dry climate due to their ability to stand the conditions inherent in this type of climate. Sedums are low-growing succulent plants of the *Crassulacea* family and are categorized as Crassulacean Acid Metabolism (CAM) plants, CAM being one of the three mechanisms for the uptake of $CO_2$ (photosynthesis) with C3 and C4. Under the CAM photosynthesis pathway, sedums can withstand long periods of heat and water stress (Carter and Butler, 2008; Durhman et al., 2006; Van Woert et al., 2005; Wolf and Lundholm, 2008) by partially closing their stomata during the day (hence reducing or inhibiting transpiration), and opening them at night to fix $CO_2$ for later use in photosynthesis. Many sedums are facultative CAM, meaning that they can switch to a C3 photosynthetic pathway when water is again available. This ability makes them very water-use efficient, which is why they are well adapted for extensive green roofs (thin layer of growing media). However this photosynthetic pathway CAM (or CAM-C3) is not parameterised in standard vegetation models (including ISBA) and even providing standard input values for this type of vegetation is a delicate task because few data have been published. Even if the lack of data did not allow for a parameterization of sedum transpiration mechanisms to be established and implemented in GREENROOF, an attempt to characterize sedums for ISBA-DF has been undertaken, bearing in mind the objective to eventually simulate the differences in characteristics and functioning inherent to the two types of vegetation commonly found on green roofs. To this end, two options for green roof vegetation have been established in GREENROOF and are provided to the user: the *GRASS* option (herbaceous lawn) and the *SEDUM* option (sedum lawn). Default characteristics for *GRASS* were already available in the standard version of ISBA-DF. A set of values was finally collected in the literature to characterize the type *SEDUM* (Table 2).

Ultimately, it is mainly the characterization of the substrate and hydrological layers which is a crucial and challenging step as the soil-forming materials implemented on green roofs are very different from the standard soils. This is discussed further in the next paragraph via a case study. The characterization of the artificial layers (Table 1) which may be added to the initial roof upon green roof implantation (such as insulation or waterproofing layers) is performed within the TEB model.

## 4 Calibration of the GREENROOF module for a standard case study

For standard applications of ISBA to natural soils and vegetation, the thermal and hydrological characteristics are deduced from empirical formulations, called pedotransfer functions, which connect these characteristics to the user-input soil texture properties (sand and clay fractions; Decharme et al., 2011). But the pedotransfer functions derived for natural soils are not really adapted to the soil-forming materials constituting the substrate or the drainage layers of a green roof. Consequently, whenever possible, it is better to directly input GREENROOF with green roof specific thermal and hydrological characteristics. However, when thermal characteristics for green roof materials are available, hydrological characteristics are not only hard to find but also consist in lab measurements which do not reflect in-situ conditions such as soil compaction or root presence/growth. Indeed, root growth results in the formation of soil micro-structures which modifies the intrinsic soil hydrological behaviour. Consequently, a calibration exercise is undertaken to best fit green roof hydrological characteristics to site conditions as well as to the GREENROOF module and thereby provide a calibration that would be adapted for the simulation of standard green roofs.

### 4.1 Case study experimental data

The GREENROOF module is evaluated against observations. This exercise is based on the experiment conducted by the Centre d'Etudes Techniques de l'Equipement de l'Est (CETE) in the North East of France near the city of Nancy. The research team at the CETE has designed an experiment with the aim of studying the relations between the thermal and hydrological characteristics of green roof systems and their thermal and hydrological behaviours for a set of vegetation/substrate/drainage layer combinations. Due to their location, the plots are exposed to a temperate oceanic climate.

The green roof plot studied, whose surface is 75 $m^2$, is composed of three natural layers of significant thicknesses (Fig. 3): a vegetation layer, a manufactured growing media (substrate) and a drainage layer underneath. In addition, the transfer of fine substrate particles into the drainage layer is prevented from by a 1.9 mm thick filter sheet which lets the water pass (geotextile material with high hydrological conductivity). In order to improve the energy performance of the building, an insulating layer of 60 mm has been installed between the base of the green roof compartment and the structural roof. Finally, two 3 mm thick waterproofing membranes on either side of the insulating layer prevent the insulator and the structural roof from water damage. The vegetation is a freshly established (2-month old) sedum lawn consisting of a mixture of seven species (*Sedum album*, *Sedum reflexum larix*, *Sedum reflexum germanium*, *Sedum spurium*, *Sedum sexangulare*, *Sedum floriferum*, and *Sedum hispanicum*, Fig. 3). The substrate, manufactured by the firm Falienor, is widely used in extensive green roof implementations. The drainage layer consists of expanded clay granules (2–10 mm grain size) manufactured by the Leca® firm. Therefore, this green roof plot is fairly representative of the green roofs which are nowadays implemented in cities.

The evolution of the thermal and hydrological status within the green roof is recorded as shown on Fig. 3. Soil temperatures are recorded using PT100 sensors at different depths near the centre of the plot including the soil surface (0, 8, 77, 85 and 128 mm). Soil water content and matrix potential are provided by a TDR probe at a single depth (66 mm), and the excess water which is drained out of the substrate and drainage layers is measured with a tipping-bucket water gauge at the base of the green roof (water outlet). In addition, a weather station based on the roof at 1.40 m above green roof surface provides air temperature, wind speed and relative humidity as well as global incoming solar radiation at a ten minute-temporal resolution. The time series available for all of these data run from 4 July to 29 November 2011.

### 4.2 Numerical setup for the case study

The calibration exercise consists of comparing the case study observations to the GREENROOF estimates obtained for a set of simulations differing in their calibration, with the aim to identify an optimal calibration for the case study green roof. Due to the difficulty in finding a large scale case study for studying green roofs, this study focuses on the scale of the green roofed building and its surrounding environment, scale at which observations are available. Consequently, simulations are carried out on one grid point. To simulate atmospheric conditions to which the green roof is exposed, a series of locally observed meteorological fields are prescribed hourly to the GREENROOF module: atmospheric pressure, shortwave incoming solar radiation (direct and diffuse), long wave incoming radiation, air temperature and relative humidity, average wind speed, and precipitation (rain and snow). The weather station installed on the greened roof provides air temperature and relative humidity, as well as average wind speed and global incoming solar radiation. The global incoming solar radiation is assumed to be about 80 % direct and 20 % diffuse. Precipitation and atmospheric pressure are provided by the nearest Météo France weather station (which is about 130 m from the green roof plot, see Fig. 3). Finally, since the infrared incoming radiation ($LW^{\downarrow}$) which must be prescribed to the model is not available in any of the two stations, it is firstly established for clear sky conditions ($LW^{\downarrow}_{\mathrm{CS}}$) according to the Stefan-Boltzmann law (Eq. 4), with air emissivity ($\varepsilon_{\mathrm{a}}$) calculated according to Prata (1996) after its temperature ($T_{\mathrm{a}}$) and humidity. Then it is modulated following Diak et al. (2000) to account for the longwave re-emission of the cloud cover ($f_{\mathrm{C}}$, Eq. (5) – assuming that the cloud temperature is equivalent to that of the surrounding air).

$$LW^{\downarrow}_{\mathrm{CS}} = \varepsilon_{\mathrm{a}}\sigma T_{\mathrm{a}}^4 \tag{4}$$

$$LW^{\downarrow} = (1 - f_C)LW^{\downarrow}_{\mathrm{CS}} + f_C\sigma T_{\mathrm{a}}^4 \tag{5}$$

where $\sigma$ is the Stefan-Boltzmann constant.

To model the studied plot with GREENROOF, the three natural layers of the roof (vegetation, substrate and drainage layer) are simulated by the ISBA-DF model while the artificial layers (the two waterproofing membranes on either sides of the insulator, and the initial structural layers of the roof) are simulated by the TEB model. Both the thermal and hydrological influences of the particle filter are considered negligible because of its low thickness and high water conductivity. Finally, to ensure numerical stability in model runs and in order to extract temperature and water content model estimates at the same vertical levels as those measured on the plot, the substrate and drainage layers were subdivided, respectively into 13 and five vertical sub layers.

### 4.3 Methodology for the initialization of green roof thermal parameters

Values for radiative and thermal characteristics (referred to as T in Table 1) of all green roof layers, be they natural or artificial, were either recovered from the technical literature (suppliers or manufacturers of similar products), or measured by Bouzouidja (in the laboratory or in-situ on the study plot) or retrieved from the scientific literature. A compilation of these values is presented in Table 3. Note that the value retained for the





GMDD
6, 1127–1172, 2013

dry soil thermal conductivity of our green roof substrate is within the range of thermal conductivities reported in Sailor et al. (2008) for eight different green roof substrates at 0 % soil moisture (0.14–0.21 $\mathrm{W\,m^{-1}\,K^{-1}}$) and this information is well correlated with the substrate density (800–851 $\mathrm{kg\,m^{-3}}$ according to Bouzouidja, 2013; Falienor, 2010). Its heat capacity is slightly above the range of those measured by Sailor et al. (2008, 950 760–1 246 000 $\mathrm{J\,m^{-3}\,K^{-1}}$) but of a similar order of magnitude.

### 4.4 Methodology for the calibration of green roof hydrological parameters

The first step of this calibration consists in compiling for each of the six hydrological characteristics needed as model inputs (referred to as H in Table 1), the values available, in the same way as for thermal parameters (technical and scientific literature, measurements). The water contents at field capacity and wilting point are prescribed from in-situ observations, leaving only four hydrological characteristics to calibrate for both the substrate and the drainage layer: the porosity, which represents the maximum interstitial space available for water; the saturated hydraulic conductivity, which corresponds to the infiltration rate of the water when the soil is saturated, the soil matrix potential at saturation, which corresponds to the pressure required to extract water from a soil matrix saturated with water; and finally the coefficient of the water retention curve used in ISBA, called $b$, which relates the matrix potential to the water content of a soil matrix according to the formulation of Clapp and Hornberger (1978). The $b$-coefficient is an empirical coefficient which varies according to soil type and can be determined by regression based on observations. This is the case for the substrate layer for which the hydrological status is continuously recorded (Fig. 3). This is done for two sets of relevant porosity-matrix potential combination and is developed in Appendix A. The hydrological characteristic values which are finally tested for calibrating GREENROOF are listed in Table 4.

Next, all possible combinations of substrate-drainage layer hydrological characteristics are established, resulting in 576 calibrated versions of the GREENROOF module. Each of them is then run and the outputs are compared against local observations to identify the best hydrological calibration to model the case study plot. The comparison of the 576 simulations focuses on the estimation of the water content recorded in the substrate. Then its impact on the green roof outlet drainage and the soil temperatures at various depths of the green roof is evaluated.

A systematic calculation of simulation statistical scores is undertaken to compare GREENROOF estimates of water content to observations, based on the Nash-Sutcliffe efficiency (NSE) and the percent bias (BIAS) (Eqs. 1 and 2 of Moriasi et al., 2007), as well as the Pearson coefficient of correlation ($R$). For the sake of visualisation, $R$ but also the centered root mean square error (RMSE), and the standard deviations (SD) of both the model and observations are all plotted on a Taylor diagram (Taylor, 2001). Finally the 576 GREENROOF simulations are compared to identify the hydrological calibration providing the best positive NSE along with the best $R$ and the smallest BIAS.

### 4.5 Determination of the best hydrological calibration for the case study

The statistical scores for the simulation of the case study substrate water content are plotted on the Taylor diagram presented in Fig. 4. Note that some simulations are showing very low statistical performance. They are the result of hydrological characteristic combinations which are not necessarily compatible with each other (and therefore do not have a physical significance), and hence are not capable of reproducing hydrologically compatible behaviours. We can see that the model performance in estimating substrate water content is acceptable. The highest correlation available is about 0.8 but this value is correlated with a SD value much higher than that of observations. Looking at NSE results for substrate water content, only four calibrations provide positive NSE values. The most meaningful statistical scores (R, NSE and BIAS) for those four calibrated-simulations, along with the associated hydrological characteristics are gathered in Table 5. The best scores are obtained for substrate and drainage layer porosities ($W_{SAT}$) of, respectively 0.674 and 0.900 $m^3 m^{-3}$, $b$-coefficients of, respectively 3.9 and 2.7, and a saturated hydraulic conductivity for the drainage layer ($k_{SAT}$)

of $3.320 \times 10^{-3}\,\mathrm{m\,s^{-1}}$. These four simulations only differ by the saturated hydraulic conductivity of the substrate and the matrix potential at saturation ($\Psi_{SAT}$) of the two layers. The NSE scores obtained (0.018 and 0.064) albeit positive are quite low but correlated with acceptable *R* of 0.73 and 0.72, and really good percent bias (respectively 1.3 % and –3.3 %). The choice of the best calibration was based primarily on the NSE value, resulting in calibrations *C* and *D* (in Table 5). Since these two calibrations only differ by very close saturated hydraulic conductivities, their statistical score are identical. As a result, we will call calibration *D* the best to facilitate the discussion hereafter. The statistics of this calibration with regard to the green roof total drainage (Table 5) is marginally better with regard to the NSE (0.08) but presents a lower correlation than for substrate water contents (*R* of 0.56) and above all a really high bias (about +130 %), suggesting that the model under-estimates the water content within the drainage layer. Another possibility for this is discussed further.

Then, the statistical scores for temperatures of the best calibration (*D* in Table 5) are good and above all better than those for the water content, with a NSE of 0.60 and 0.64, respectively for the bottoms of the substrate (77 mm) and the drainage layer (128 mm). These values are correlated with a good *R* (0.93 and 0.91) and a positive bias, with the bias getting smaller when looking deeper in the green roof (2.12 °C at 77 mm versus 0.57 °C at 128 mm; similar for other depths but not shown). These better results in NSE and *R* for temperatures than for substrate water content can be explained by the fact that thermal transfers are less complex, hence easier to model, than hydrological ones. Secondly the soil temperatures are quite sensitive to atmospheric forcings that have a daily cycle.

Finally, the best set of hydrological characteristics for modelling the in-situ behaviour of the green roof studied with GREENROOF is that displayed in Table 5 for calibration *D*. The porosity of the substrate is equal to that provided by the supplier while that of the drainage layer corresponds to the technical and scientific literature. The saturated hydraulic conductivities provided by the supplier or measured by Bouzouidja (2013) are equally efficient. The value for the *b*-coefficient is surprising because it does





GMDD
6, 1127–1172, 2013

not correspond to that obtained for the porosity of that calibration (see Table 4, Appendix A). The best calibration obtained for the drainage layer whose texture, porosity and hydrological behaviour are complex eventually displays hydrological characteristics which are typical of the behaviour of peat: high porosity and saturated hydraulic conductivity matched to a low *b*-coefficient (according to Lawrence and Slater, 2008). This information is an interesting outcome because it allows one to relate the hydrological behaviour of expanded clay granules to a better known soil component.

### 4.6 Evolution of green roof hydrological and thermal performance after model calibration

The evolution of the substrate water content and the green roof drainage over the time series available (between July and November 2011) are presented on Fig. 5 for the four best calibrations to illustrate their discrepancies in relation to that of their statistical scores. GREENROOF reproduces quite well the dynamics and magnitude of the water content in the substrate layer, although maxima are frequently over-estimated by the model. The model fit with the substrate observations seems to be better at the beginning and at the end of the time serie studied. For the outlet drainage (Fig. 5), which combines the behaviours of both the substrate and the drainage layers, the correlation between the model and the observations is clearly not as good. Looking at best calibration *D*, the bias of GREENROOF on the outlet drainage over the entire time serie (+129.7 %) represents a volume of water of 3.62 $m^3$, with 2.79 $m^3$ recorded and 6.41 $m^3$ simulated by the model. Firstly, this bias is explained by the fact that the model always simulates a background drainage at the green roof base even when none is observed in reality. This contribution may be small amounts at each time step but represents 1.64 $m^3$ over the 5-months period, in other words nearly half of the bias. Secondly, the high positive bias in the outlet drainage is likely to be related to the presence of a device with stoppers, which is installed between the green roof base and the tipping-bucket water gauge. This device allows a water blade of varying height to be retained, when it exists, by using stoppers placed at different heights of the outlet (multiple of 15 mm). It consists in an experimental set up, which is not a device generally implemented on green roofs. It is intended to keep water on the roof for use during dry spells or to delay and reduce roof run off peaks during heavy rainfall events. Obviously, this device, which is not modelled in GREENROOF, complicates the analysis of the calibration exercise presented herein since it prevents part of the water that is drained out of the drainage layer to be recorded. As the dates at which these stoppers were installed (as well as their numbers) are known, the bias in outlet drainage has been calculated for two time periods, between 10/07 and 08/08 and between 28/10 and 29/11 (two stoppers), and between 09/08 and 27/10 (one stopper). If related to the amount of precipitation to which the green roof has been exposed, the resulting biases are, respectively 0.018 and 0.008 in $m^3$ of water per mm of rain, showing that the model correlates better with observations when fewer stopper are installed. These results suggest that GREENROOF should be capable of better simulating green roof outlet drainage without any stopper in place. Nevertheless, it presents a general tendency to overestimate the outlet drainage, as can be seen especially at the beginning of the simulation. This suggests that GREENROOF probably underestimates the water content in the drainage layer. Unfortunately, this behaviour can not be evaluated against observations since, for technical reasons, the moisture status is not recorded in this layer.

The evolution of recorded and simulated (calibration *D*) green roof temperatures, is presented Fig. 6. Be it at the bottom of the substrate (at 77 mm) or the drainage layer (at 128 mm), the temperatures estimated by GREENROOF demonstrate a good correlation with those observed, especially at the beginning of the time serie studied (until mid-August). By contrast, the amplitude of the temperatures simulated by GREENROOF is greater than that of observations, even if the model is able to captures seasonal amplitudes. This is confirmed by standard deviation values for the substrate and drainage layer temperatures of, respectively 7.7 °C and 7.3 °C compared to 5.9 °C and 5.5 °C in observations. For the substrate layer, the model tends to overestimate the temperature (with a bias of 2.12 °C), although this is less true at the beginning of the simulation.





GMDD
6, 1127–1172, 2013

This is partially due to the fact that the water content is underestimated by the model in that layer. This has consequences on the calculation of the effective thermal properties of the soil matrix which are calculated according to Peters-Lidard et al. (1998) based on the dry thermal properties shown in Table 3, the porosity and the water content of the soil matrix. Eventually, an underestimated water content will generate lower than in reality thermal conductivity and heat capacity, with a consequent increase in the soil matrix temperature. The same behaviour applies to the drainage layer. Nevertheless the model bias, even if positive over the time serie studied, is smaller for this layer (0.57 °C). It is noticeable on Fig. 6 that, from around 01/11, the model starts to underestimate the temperatures in that layer. The bottom of the drainage layer being the one the most influenced by the changes in temperatures inherent to the structural building, the negative bias observed at the end of the simulation is likely to be due to the setting of a too low heating trigger temperature compared to the reality.

## 5 Conclusions and perspectives

A parameterization called GREENROOF for simulating extensive green roofs across the city has been developed within TEB, that is consistent with the modular architecture of SURFEX. While the natural surface scheme ISBA-DF simulates the transfers of heat and water within the natural compartments of the green roof, TEB handles transfers within artificial layers of the green roof and the structural roof. The GREENROOF module consists of the coupling of these two models via the heat flux which establishes between the natural and artificial roof layers in contact as well as a set of specific soil-forming materials characteristics. A vertical green roof design as well as two greening options (grass or sedum lawn) are available. In order to identify the soil-forming characteristics that best describe green roof thermal and hydrological behaviours within GREENROOF, a calibration exercise is realized for a case study, an experimental green roof plot located in the North East of France. Results show that the GREENROOF module performs well in reproducing the dynamics of water contents throughout the green roof and is acceptable with regard to their amplitude. The differences observed between modelled and observed water contents do not impact too much the simulation of temperatures which presents good statistical scores. Due to the thermal inertia of the substrate and drainage layers, the scores for temperatures are, as expected, better when looking deeper in the natural green roof compartment, which allows for a good thermal coupling with the artificial/structural roof layers. Based on the hypothesis that the experimental plot studied (extensive, sedum mixture lawn, typical substrate and drainage layer materials) is a type of green roof that is frequently implemented on urban buildings, the set of hydrological characteristics determined via the case study is retained to simulate green roofs at the scale of cities.

The GREENROOF module will allow the impacts of green roof implementation on various types of buildings (1-D with atmospheric forcings) and at city-scale (forced with atmospheric fields or coupled to an atmospheric model) to be modelled. The coupled developments of the GREENROOF module and the Building Energy Model (BEM, Bueno et al., 2012) within TEB will assess the potential of green roofs (and associated water resources) as a sustainable adaptation strategy for cities in terms of indoor thermal comfort and energy consumption, as well as urban heat island mitigation if coupled to an atmospheric model. Through the various options currently available in ISBA other impacts of green roofs could be studied at the scale of cities, such as for example their potential for carbon dioxide sequestration.

Future developments of this work should include the analysis of a green roof plot with similar combination of vegetation and substrate but with a retention layer instead of a drainage layer. It would help in refining a calibration for modelling green roofs that have such an hydrological function, although the current parameterization has already demonstrated its ability to reproduce this function quite well. Also, the way the source code of GREENROOF has been developed will allow one to take advantage of any future developments that the ISBA model source code will benefit from. Practically, the GREENROOF module has been implemented within the version 7.3 of the SURFEX platform. For further details, including how to obtain a copy of the source code, see http://www.cnrm.meteo.fr/surfex/.

# Appendix A

## Fitting b-coefficient of the water retention curve to observations

### A1 Method

The *b*-coefficient is involved in a formulation implemented in ISBA (hence called by the GREENROOF module) which connects the water potential to the water content in a soil matrix, derived by Clapp and Hornberger (1978):

$$\frac{\psi}{\psi_{\mathrm{SAT}}} = \left(\frac{\mathrm{wc}}{\mathrm{wc}_{\mathrm{SAT}}}\right)^{-b} \tag{A1}$$

where $\psi$ (m) is the water potential for a specific water content wc ($\mathrm{m^3\,m^{-3}}$), $\psi_{\mathrm{SAT}}$ (m) is the water potential at saturation corresponding to the water content at saturation (i.e. the porosity) $\mathrm{wc}_{\mathrm{SAT}}$ ($\mathrm{m^3\,m^{-3}}$) and $b$ is an empirical coefficient, which must be estimated. This formulation when plotted for a soil is called the water retention curve. Following formulation (A1), the *b*-coefficient can be estimated, if observations are available, as the opposite of the slope of the water retention curve expressed as :

$$\log_{10}\left(\frac{\psi}{\psi_{\mathrm{SAT}}}\right) = -b \times \mathrm{LOG}_{10}\left(\frac{\mathrm{wc}}{\mathrm{wc}_{\mathrm{SAT}}}\right) \tag{A2}$$

Note that for applications of ISBA to natural soils, the *b*-coefficient does not need to be user-calibrated because it is estimated within the model after pedotransfer functions based on user-input soil texture (sand and clay fractions). The case of green roof soil-forming materials is different because sand and clay fractions are not really appropriate





GMDD
6, 1127–1172, 2013

to characterize them. Hence, for the substrate of the green roof studied for which water contents and matrix potentials were recorded between July and November 2011, the *b*-coefficient can be estimated.

### A2 Fitting *b*-coefficients for the case study green roof substrate

The *b*-coefficient has been estimated based on formulation (A2) using a linear regression for two compatible combinations of porosity and saturated water potential tested in the calibration exercise, respectively 0.674 $m^3\,m^{-3}$ with −0.1 m for the first combination and 0.411 $m^3\,m^{-3}$ with −0.1 m for the second combination. For the first combination, the linear regression resulted in a fitted *b*-coefficient of 2.9. The same treatment for the second combination (Fig. A2) resulted in a fitted *b*-coefficient of 3.9. The two resulting water retention curves are displayed on Figs. A1 and A2, showing the agreements between the *b*-fitted theoretical curves and the observed curves. For both combinations, the agreement is acceptable but the Clapp and Hornberger (1978) formulation does not seem able to reproduce the tail of the observed water retention curve – when water content is above 0.20/0.25 $m^3\,m^{-3}$. Also, the second combination appears better than the first at reproducing the inflexion of the observed curve, although it does not capture the points with the lowest water contents/greatest matrix potentials. However, the functioning of water potential probes can be well altered in dry conditions because of the rough texture (and the resulting lack of contact) of the soil-forming material of the green roof substrate. This may question the validity of the high water potential recorded on that green roof plot.

*Acknowledgements.* The results presented in this publication are the outcome of two research projects: MUSCADE (Modélisation Urbaine et Stratégie d'adaptation au Changement climatique pour Anticiper la Demande et la production Énergétique, ANR-09-VILL-0003) and Veg-DUD (Rôle du végétal dans le Développement Urbain Durable, ANR-09-VILL-0007). We are grateful for the expertise and support provided by Aaron Boone and Bertrand Decharme (CNRM-GAME) on the ISBA-DF model.

The publication of this article is financed by CNRS-INSU.

## References


ACERMI (Association pour la CERtification des Matériaux Isolants: CSTB – LNE): CERTIFICAT ACERMI No. 04/003/323, Licence no. 04/003/323, 2009.

ARGEX: http://www.argex.eu/en/products/characteristics.html, last access: 24 February 2012.

Alexandri, E. and Jones, P.: Developing a one-dimensional heat and mass transfer algorithm for describing the effect of green roofs on the built environment: comparison with experimental results, Build. Environ., 42, 2835–2849, doi:10.1016/j.buildenv.2006.07.004, 2007.

Bass, B. and Baskaran, B.: Evaluating Rooftop and Vertical Gardens as an Adaptation Strategy for Urban Areas, Report no. NRCC-46737, edited by: National Research Council Canada, Institute for Research in Construction, Ottawa (Canada), 2003.

Bass, B., Krayenhoff, E. S., Martilli, A., Stull, R. B., and Auld, H.: The impact of green roofs on Toronto's urban heat island, in: Proceedings of the First North American Green Roof Conference: Greening Rooftops for Sustainable Communities, 20–30 May, Chicago, Toronto (Canada), Cardinal Group, 292–304, 2003.

Berghage, R., Beattie, D., Jarrett, A., Thuring, C., and Razaei, F.: Green Roofs for Stormwater Runoff Control, Report no. EPA/600/R-09/026, February 2009, edited by the National Risk Management Research Laboratory, Office of Research and Development, US Environment Protection, Agency, Cincinnati, OH 45268, 2009.

Berndtsson, J. C., Bengtsson, L., and Jinno, K.: Runoff water quality from intensive and extensive vegetated roofs, Ecol. Eng., 35, 369–380, 2009.

BING (Federation of European Rigid Polyurethane Foam Associations): Thermal insulation materials made of rigid polyurethane foam (PUR/PIR). Properties – Manufacture, Report no. 1, 6 October 2006, available at: www.excellence-in-insulation.eu/site/fileadmin/

user_upload/PDF/library/reports/BING_TECH_REP_on_Thermal_insulation_materials_made_of_rigid_polyurethane_foam.pdf, (last access: 14 February 2013), 2006.

Boone, A., Masson, V., Meyers, T., and Noilhan, J.: The influence of the inclusion of soil freezing on simulations by a soil-vegetation-atmosphere transfer scheme, J. Appl. Meteorol., 39, 1544–1569, 2000.

Bouzouidja, R.: Caractérisation du substrat d'une toiture végétalisée, Master's thesis, University of Lorraine, Nancy, France, 2010.

Bouzouidja, R., Lacroix, D., Séré, G., and Claverie, R.: Experimental determination of hydrological parameters of green roofs, Build. Environ., in preparation, 2013.

Bueno, B., Pigeon, G., Norford, L. K., Zibouche, K., and Marchadier, C.: Development and evaluation of a building energy model integrated in the TEB scheme, Geosci. Model Dev., 5, 433–448, doi:10.5194/gmd-5-433-2012, 2012.

Carter, T. and Butler, C.: Ecological impacts of replacing traditional roofs with green roofs in two urban areas, Cities Environ., 1, 9, 2008.

Castletown, H. F., Stovin, V., Beck, S. B. M., and Davison, J. B.: Green roofs; building energy savings and the potential for retrofit, Energ. Buildings, 41, 1582–1591, 2010.

Clapp, R. B. and Hornberger, G. M.: Empirical equations for some soil hydraulic properties, Water Resour. Res., 14, 601–604, 1978.

CRITT Horticole (Centre régional pour l'Innovation et le Transfert Technologique Horticole): Définition et mesure du LAI. Intégration de la résistance stomatique (RS) dans la formule de l'ETP, Unpublished report, 2012.

de Munck, C., Pigeon, G., Masson, V., Meunier, F., Bousquet, P., Tréméac, B., Merchat, M., Poeuf, P., and Marchadier, C.: How much air conditioning can increase air temperatures for a city like Paris (France)?, Int. J. Climatol., 33, 210–227, doi:10.1002/joc.3415, 2013.

Decharme, B., Boone, A., Delire, C., and Noilhan, J.: Local evaluation of the interaction between soil biosphere atmosphere soil multilayer scheme using four pedotransfer functions, J. Geophys. Res., 116, D20126, 1–29, doi:10.1029/2011JD016002, 2011.

Del Barrio, E. P.: Analysis of the green roofs cooling potential in buildings, Energ. Buildings, 27, 179–193, 1998.

Diak, G. R., Bland, W. L., Mecikalski, J. R., and Anderson, M. C.: Satellite-based estimates of longwave radiation for agricultural applications, Agr. Forest Meteorol., 103, 349–355, doi:10.1016/S0168-1923(00)00141-6, 2000.

Doya, M., Briottet, X., Djedjig, R., and Ouldboukhitine, S.: Description des mesures VEGDUD du 23 September 2011, unpublished report, 2011.

Durham, A. K., Rowe, D. B., and Rugh, C. L.: Effect of watering regimen on chlorophyll fluorescence and growth of selected green roof plant taxa, HortScience, 41, 1623–1628, 2006.

EEA: European Environment Agency: Urban adaptation to climate change in Europe. Challenges and opportunities for cities together with supportive national and European policies, EEA Report no 2/2012, ISSN 1725–9177, 2012.

Falienor: Résultats de l'analyse de substrat de toiture végétalisée No. 1807676 – 14-F TOITURE par le Laboratoire SAS, issued on 9 March 2010.

Farouki, O. T.: Thermal properties of soils, Ser. on Rock and Soil Mech., 11, Trans. Tech. Publ., Clausthal-Zellerfled, Germany, 136 pp., 1986.

Foster, J., Lowe, A., and Winkelman, S.: The value of green infrastructure for urban climate adaptation, Published by the Center for Clean Air Policy, Washington DC, USA, February 2011.

Getter, K. L. and Rowe, D. B.: The role of extensive green roofs in sustainable development, HortScience, 41, 1276–1285, 2006.

Giguère, M.: Mesures de lutte aux îlots de chaleur urbains. Revue de literature, Direction des risques biologiques, environnementaux et occupationnels, Institut National de Santé Publique, Gouvernement du Québec, Québec (Québec, Canada), Juillet 2009.

Gill, S. E., Handley, J. F., Ennos, A. R., and Pauleit, S.: Adapting cities for climate change: the role of the green infrastructure, Built Environ., 33, 115–133, 2007.

Hamdi, R., and Masson, V.: Inclusion of a drag approach in the town energy balance (TEB) scheme: offline 1D evaluation in a street canyon, J. Appl. Meteorol. Clim., 47, 2627–2644, doi:10.1175/2008JAMC1865.1, 2008.

Hilten, R. N., Lawrence, T. M., and Tollner, E. W.: Modeling stormwater runoff from green roofs with HYDRUS-1D, J. Hydrol., 358, 288–293, 2008.

Jacquet, S.: Performance énergétique d'une toiture végétale au centre-ville de Montréal, Résumé de mémoire, Centre d'Ecologie Urbaine de Montréal, ISBN 978-2-9810129-8-2, available at:http://www.ecologieurbaine.net/node/1214, (last access: 14 February 2013), 2011.

Jaffal, I., Ould-Boukhitine, S.-E., and Belarbi, R.: A comprehensive study of the impact of green roofs on building energy performance, Renew. Energ., 43, 157–164, 2012.

Jim, C. Y.: Effect of vegetation biomass structure on thermal performance of tropical green roof, Landscape Ecol. Eng., 8, 173–187, doi:10.1007/s11355-011-0161-4, 2011.
Jim, C. Y. and He, H.: Coupling dynamics with meteorological conditions in the green roof ecosystem, Ecol. Eng., 36, 1052–1063, 2010.
Jim, C. Y. and Peng, L. L. H.: Weather effect on thermal and energy performance of an extensive tropical green roof, Urban For. Urban Gree., 11, 73–85, 2011.
Jim, C. Y. and Tsang, S. W.: Modeling the heat diffusion process in the abiotic layers of green roofs, Energ. Buildings, 43, 1341–1350, 2011.
Kalzip®: Kalzip low U-value roof system – achieving 0.10 W/m$^2$/K, Product review, available at: www.kalzip.com/PDF/uk/Kalzip-low-U-value-system.pdf, (last access: 14 February 2013), 2010.
Kumar, R. A. and Kaushik, S. C.: Performance evaluation of green roof and shading for thermal protection of buildings, Build. Environ., 40, 1505–1511, 2005.
Lawlor, G., Currie, B. A., Doshi, H., and Wieditz, I.: Green roofs: a resource manual for municipal policy makers, Report 65255, Published by Canada Mortgage and Housing Corporation, Ottawa (Ontario, Canada), May 2006.
Lawrence, D. M. and Slater, A. G.: Incorporating organic soil into a global climate model, Clim. Dynam., 30, 145–160, 2008.
Lazzarin, R. M., Castellotti, F., Busato, F.: Experimental measurements and numerical modelling of a green roof, Energ. Buildings, 37, 1260–1267, 2005.
Leca®: Declaration of technical specifications BS EN 13055-1 for lightweight aggregate, issued on 1 January 2009.
Leca®: http://www.leca.co.uk/33755, last access: 24 February 2012.
Lemonsu, A. and Masson, V.: Simulation of a summer urban breeze over Paris, Bound.-Lay. Meteorol., 104, 463–490, 2002.
Lemonsu, A., Grimmond, C. S. B., Masson, V.: Modeling the surface energy balance of the core of an old Mediterranean city: Marseille, J. Appl. Meteorol., 43, 312–327, 2004.
Lemonsu, A., Bélair, S., Mailhot, J., Leroyer, S.: Evaluation of the town energy balance model in cold and snowy conditions during the Montreal Urban Snow Experiment 2005, J. Appl. Meteorol. Climatol., 49, 346–362, 2010.
Lemonsu, A., Pigeon, G., Marchadier, C., and Salagnac, J.-L.: Research report for the VURCA project, Scénarios du bâti & simulations, No ANR-08-VULCN-013 VURCA, 47 pp., 2011.

Lemonsu, A., Masson, V., Shashua-Bar, L., Erell, E., and Pearlmutter, D.: Inclusion of vegetation in the Town Energy Balance model for modelling urban green areas, Geosci. Model Dev., 5, 1377–1393, doi:10.5194/gmd-5-1377-2012, 2012.

Masson, V.: A physically-based scheme for the urban energy budget in atmospheric models, Bound.-Lay. Meteorol., 94, 357–397, 2000.

Masson, V., Champeaux, J. L., Chauvin, F., Meriguet, C., and Pigeon, G.: ECOCLIMAP: a global database of land surface parameters at 1-km resolution in meteorological and climate models, J. Climate, 16, 1261–1282, 2003.

Masson, V., Le Moigne, P., Martin, E., Faroux, S., Alias, A., Alkama, R., Belamari, S., Barbu, A., Boone, A., Bouyssel, F., Brousseau, P., Brun, E., Calvet, J.-C., Carrer, D., Decharme, B., Delire, C., Donier, S., Essaouini, K., Gibelin, A.-L., Giordani, H., Habets, F., Jidane, M., Kerdraon, G., Kourzeneva, E., Lafaysse, M., Lafont, S., Lebeaupin Brossier, C., Lemonsu, A., Mahfouf, J.-F., Marguinaud, P., Mokhtari, M., Morin, S., Pigeon, G., Salgado, R., Seity, Y., Taillefer, F., Tanguy, G., Tulet, P., Vincendon, B., Vionnet, V., and Voldoire, A.: The SURFEXv7.2 land and ocean surface platform for coupled or offline simulation of Earth surface variables and fluxes, Geosci. Model Dev. Discuss., 5, 3771–3851, doi:10.5194/gmdd-5-3771-2012, 2012.

Mentens, J., Raes, D., and Hermy, M.: Green roofs as a tool for solving the rainwater runoff problem in the urbanized 21st century?, Landscape Urban Plan., 77, 217–226, 2006.

Moriasi, D. N., Arnold, J. G., Van Liew, M. W., Bingner, R. L., Harmel, R. D., and Veith, T. L.: Model evaluation guidelines for systematic quantification of accuracy in watershed simulations, T. ASABE, 50, 885–900, 2007.

Mualem, Y.: A new model to predicting the hydraulic conductivity of unsaturated porous media, Water Resour. Res., 12, 513–522, 1976.

Nardini, A., Andri, S., and Crasso, M.: Influence of substrate depth and vegetation type on temperature and water runoff mitigation by extensive green roofs: shrubs versus herbaceous plants, Urban Ecosyst., 15, 697–708, doi:10.1007/s11252-011-0220-5, 2012.

Noilhan, J. and Planton, S.: A simple parameterization for land surface processes for meteorological models, Mon. Weather Rev., 117, 536–549, 1989.

Oberndorfer, E., Lundholm, J., Bass, B., Coffman, R. R., Doshi, H., Dunnett, N., Gaffin, S., Kohler, M., Liu, K. K. Y., and Rowe, B.: Green roofs as urban ecosystems: ecological structures, functions, and services, BioScience, 57, 823–833, 2007.

Ochs, F., Heidemann, W., and Müller-Steinhagen, H.: Effective thermal conductivity of the insulation of high temperature underground thermal stores during operation, in: Proceedings of the Ecostock 2006 conference, Richard Stockton College, New Jersey, USA, 31 May–2 June 2006.

Offerle, B., Grimmond, C. S. B., and Fortuniak, K.: Heat storage and anthropogenic heat flux in relation to the energy balance of a central European city centre, Int. J. Climatol., 25, 1405–1419, 2005.

Ould-Boukhitine, S.-E., Belarbi, R., Jaffal, I., and Trabelsi, A.: Assessment of green roof thermal behaviour: a couple heat and mass transfer model, Build. Environ., 46, 2624–2631, doi:10.1016/j.buildenv.2011.06.021, 2011.

Palla, A., Gnecco, I., and Lanza, G.: Unsaturated 2D modelling of subsurface water flow in the coarse-grained porous matrix of a green roof, J. Hydrol., 379, 193–204, 2009.

Palla, A., Gnecco, I., and Lanza, G.: Compared performance of a conceptual and a mechanistic hydrologic models of a green roof, Hydrol. Process., 26, 73–84, 2012.

Penney, J.: Climate change adaptation in the city of Toronto, Lessons for Great Lakes communities, Clean Air Partnership, Toronto, Ontario, Canada, December 2008, available at: www.cleanairpartnership.org/.

Peters-Lidard, C. D., Blackburn, E., Lian, X., and Wood, E. F.: The effect of soil thermal conductivity parameterization on surface energy fluxes and temperatures, J. Atmos. Sci.,55, 1209–1224, doi:10.1175/1520-0469(1998)055<1209:TEOSTC>2.0.CO;2, 1998.

Pigeon, G., Moscicki, M. A., Voogt, J. A., and, Masson, V.: Simulation of fall and winter surface energy balance over a dense urban area using the TEB scheme, Meteorol. Atmos. Phys., 102, 159–172, 2008.

Prata, A. J.: A new long-wave formula for estimating downward clear-sky radiation at the Surface, Q. J. R. Meteorol. Soc., 122, 1127–1151, 1996.

RECTICEL®: http://www.recticelinsulation.fr/nos-produits/powerline/#donnees_techniques, last access: 1 June 2012.

Rosenzweig, C., Solecki, W. D., Parshall, L., Lynn, B., Cox, J., Goldberg, R., Hodges, S., Gaffin, S., Slosberg, R. B., Savio, P., Dunstan, F., and Watson, M.: Mitigating New York City's Heat Island. Integrating stakeholder perspectives and scientific evaluation, B. Am. Meteorol. Soc., 90, 1297–1312, 2009.

Sailor, D. J.: A green roof model for building energy simulation programs, Energ. Buildings, 40, 1466–1478, 2008.





Title Page
Abstract | Introduction
Conclusions | References
Tables | Figures
◀| |▶
◀ ▶
Back | Close
Full Screen / Esc
Printer-friendly Version
Interactive Discussion

SILRES®: www.wacker.com/cms/media/publications/downloads/6528_EN.pdf, last access: 24 February 2012.

Simunek, J., Voel, T., amd Van Genuchten, M.Th.: The SWMS_2D code for simulating water flow and solute transport on two-dimensional variably saturated media, Version 1.21., Research report No. 132, US Salinity Laboratory, USDA, ARS, Riverside, California, 197 pp., 1994.

Simunkek, J., Van Genuchten, M. Th., and Sejna, M.: The HYDRUS_1D Software package for simulating the one-dimensional movement of water, heat and multiple solutes in variably-saturated media, Version 3.0, HYDRUS Software Series 1. Dept. of Environmental Science, University of California Riverside, Riverside, California, USA, 240 pp., 2005.

Sinclair: http://www.william-sinclair.co.uk/industrial/products/expanded_clay, last access: 24 February 2012.

SOPREMA®: SOPRALENE® FLAM JARDIN. Fiche technique No. DT-10/005_FR CE, published by SOPREMA (Strasbourg, France), 2012a.

SOPREMA®: SOPRALENE® FLAM 180. Fiche technique No DT-09/086_FR CE, published by SOPREMA (Strasbourg, France), 2012b.

Taylor, K. E.: Summarizing multiple aspects of model performance in a single diagram, J. Geophys. Res., 106, 7183–7192, 2001.

USEPA: Reducing Urban Heat Islands: Compendium of Strategies. Green Roofs, 26 pp., available at: http://www.epa.gov/hiri/mitigation/greenroofs.htm, (last access: 14 February 2013), 2008.

Van Genuchten, M. Th.: A closed-form equation for predicting the hydraulic conductivity of unsaturated soils, Soil Sci. Soc. Am. J., 44, 892–898, 1980.

Van Woert, N. D., Rowe, D. B., Andresen, J. A., Rugh, C. L., and Xiao, L.: Watering regime and green roof substrate design affect Sedum plant growth, HortScience, 40, 659–664, 2005.

Voyde, E., Fassman, E., Simcock, R.: Hydrology of an extensive living roof under sub-tropical climate conditions in Auckland, New Zealand, J. Hydrol., 394, 384–395, 2010.

Wark, C. G. and Wark, W. W.: Green roof specifications and standards. Establishing an emerging technology, Construct. Spec., 56, August 2003, no 8, , available at: www.proenviroconstruction.com/pdf/GreenRoof.pdf, (last access: 14 February 2013), 2003.

Wolf, D. and Lundholm, J. T.: Water uptake in green roof microcosms: effects of plant species and water availability, Ecol. Eng., 33, 179–186, 2008.

Yu, C. and Zheng, C.: HYDRUS: software for flow and transport modeling in variably saturated media, Ground Water, 48, 787–791, 2010.





GMDD

6, 1127–1172, 2013

The GREENROOF module (v7.3) for TEB

C. S. de Munck et al.

**Table 1.** GREENROOF model input parameters (T and H refer, respectively to a Thermal and a Hydrological parameter).

| | Parameter (unit) |
|---|---|
| Design | Fraction of structural roof vegetated (–)<br>Number of green roof sub-layers used for calculation and their respective depths (m) |
| Vegetation | Type (herbaceous lawn or sedum lawn)<br>Fraction of vegetation covering the vegetated ground (–)<br>LAI (–)<br>Albedo (–)<br>Emissivity (–)<br>Minimum stomatal resistance ($s\,m^{-1}$)<br>Roughness length for momentum (m) |
| Substrate and hydrological control sub-layers | Initial soil moisture (soil water index) for surface, root layers and hydrological sub-layers<br>Initial soil-forming material temperature for surface, root layers and hydrological sub-layers |
| Substrate and hydrological control sub-layers | T: Dry soil thermal conductivity ($W\,m^{-1}\,K^{-1}$)<br>T: Dry soil heat capacity ($J\,m^{-3}\,K^{-1}$)<br>H: Porosity ($m^3\,m^{-3}$)<br>H: Saturated hydraulic conductivity ($m\,s^{-1}$)<br>H: Matrix potential at saturation (m)<br>H: *b*-coefficient for water retention curve (–)<br>H: Water content at field capacity ($m^3\,m^{-3}$)[a]<br>H: Water content at wilting point ($m^3\,m^{-3}$)[a] |
| Artificial layers added to the structural roof (TEB) | Total number of layers of the artificial roof and their respective thicknesses (m)<br>Albedo of the top artificial layer (–)<br>Emissivity of the top artificial layer (–)<br>Thermal conductivity ($W\,m^{-1}\,K^{-1}$)<br>Heat capacity ($J\,m^{-3}\,K^{-1}$) |

[a] For hydrological control sub-layers, only used to initialize water contents.





GMDD
6, 1127–1172, 2013
The GREENROOF module (v7.3) for TEB
C. S. de Munck et al.

**Table 2.** Vegetation characteristics for SEDUM compared to that of GRASS (defined according to the default values proposed by Masson et al., 2003).

| GREENROOF parameter (unit) | Value (GRASS) | Value (SEDUM) | Method for SEDUM (Source) |
|---|---|---|---|
| Fraction of vegetation covering the ground (–) | 0.9 | 0.9 | Chosen identical to that of GRASS |
| Leaf Area Index (–) | 2 | 3 | Measured (CRITT Horticole, 2012) |
| Long wave albedo (–) | 0.300 | 0.154 | Measured (Doya, 2011) |
| Shortwave albedo (–) | 0.100 | 0.154 | Measured (Doya, 2011) |
| Emissivity (–) | 0.95 | 0.83 | Measured (Feng et al., 2010) |
| Minimal stomatal resistance ($\mathrm{s\,m^{-1}}$) | 40 | 150 | Chosen higher than that for GRASS (Sect. 3.3) |
| Roughness length for momentum (m) | 0.01 | 0.01 | Chosen identical to that of GRASS |

**Table 3.** General and thermal characteristics of green roof substrate, drainage layers and roof artificial layers (values in bold are used in simulations).

| | Characteristics (unit) | Value | Method (source) |
|---|---|---|---|
| SUBSTRATE | Thickness (m) | **0.08** | Measured (Bouzouidja, 2012) |
| | Dry unit weight of soil particles (kg m$^{-3}$) | 2610 | Deducted from Falienor (2010) |
| | Dry soil thermal conductivity (W m$^{-1}$ K$^{-1}$) | **0.15** | Measured[a] (Bouzouidja, 2010) |
| | Dry soil heat capacity (J m$^{-3}$ K$^{-1}$) | **1 342 000** | Measured[b] (Bouzouidja, 2010) |
| DRAINAGE | Thickness (m) | **0.05** | Measured (Bouzouidja, 2012) |
| | Dry unit weight of soil particles (kg m$^{-3}$) | 570 | Supplier information (Leca®, 2009) |
| | Dry soil thermal conductivity (W m$^{-1}$ K$^{-1}$) | < 0.11<br>0.125<br>0.113<br>0.075–**0.090** | Supplier information (Leca®, 2009)<br>Manufacturer information (SILRES®, 2012)<br>Manufacturer information (Sinclair, 2012)<br>Ochs et al. (2006) |
| | Dry soil heat capacity (J m$^{-3}$ K$^{-1}$) | **331 500** | Deducted from manufacturer information (Sinclair, 2012) according to density |
| ARTIFICIAL | Material / function<br><br>*5 layers, from top (1) to bottom (5)* | (1) waterproofing membrane<br>(2) insulating sheet (PIR[c])<br>(3) waterproofing membrane<br>(4) insulator<br>(5) concrete | (1) Supplier information (SOPREMA®, 2012a)<br>(2) ACERMI (2009)<br>(3) Supplier information (SOPREMA®, 2012b)<br>(4 to 5) Deducted from building type and age (Lemonsu et al., 2011) |
| | Thickness (m) | (1) **0.003**<br>(2) **0.060**<br>(3) **0.003**<br>(4) **0.10**<br>(5) **0.20** | (1) Supplier information (SOPREMA®, 2012a)<br>(2) Supplier information (RECTICEL®, 2012)<br>(3) Supplier information (SOPREMA®, 2012b)<br>(4 and 5) Deducted from building type and age (Lemonsu et al., 2011) |
| | Thermal conductivity (W m$^{-1}$ K$^{-1}$) | (1) **0.7**<br>(2) **0.024**<br>(3) **0.7**<br>(4) **0.035**<br>(5) **2.3** | (1 and 3) Deducted from building type and age (Lemonsu et al., 2011)<br>(2) ACERMI (2009)<br>(4 and 5) Deducted from building type and age (Lemonsu et al., 2011) |
| | Heat capacity (J m$^{-3}$ K$^{-1}$) | (1) **2 100 000**<br>(2) **44 800**<br>(3) **2 100 000**<br>(4) **75 000**<br>(5) **2 300 000** | (1 and 3) Deducted from building type, age and usage (Lemonsu et al., 2011)<br>(2) Deducted from BING (2006) and Kalzip® (2010) based on density (RECTICEL®, 2012)<br>(4 and 5) Deducted from building type, age and usage (Lemonsu et al., 2011) |

[a] For a similar substrate, mean between −10 and 50 °C.
[b] For a similar substrate, at 20 °C.
[c] PolyIsocyanuRate foam with aluminium layer.

GMDD

6, 1127–1172, 2013

The GREENROOF module (v7.3) for TEB

C. S. de Munck et al.





**Table 4.** Hydrological characteristics tested for green roof calibration exercise.

| | Characteristics (unit) | Value | Method (Source) |
|---|---|---|---|
| SUBSTRATE | Porosity ($m^3\,m^{-3}$) | **0.674**<br>**0.411** | Supplier information (Falienor, 2010)<br>Measured (Bouzouidja, 2012) |
| | Saturated hydraulic conductivity ($m\,s^{-1}$) | **$1.073 \times 10^{-3}$**<br>**$2.162 \times 10^{-3}$** | Supplier information (Falienor, 2010)<br>Measured (Bouzouidja, 2012) |
| | Matrix potential at saturation (m) | **–0.932**<br>**–0.10** | Deducted from observations<br>Value fitted on observed water retention curves (Appendix A) |
| | *b*-coefficient for water retention curve (–) | **2.9**<br><br>**3.9** | Deducted from water retention curve (Fig. A1) porosity of 0.674 and matrix potential of −0.10<br>Deducted from water retention curve (Fig. A2) with porosity of 0.411 and matrix potential of −0.10 |
| | Water content at field capacity | **0.37** | Deducted from observations |
| | Water content at wilting point ($m^3\,m^{-3}$) | **0.15** | Deducted from observations |
| DRAINAGE | Porosity ($m^3\,m^{-3}$) | **0.553**<br>**0.9** | Deducted from supplier density data (Table 3)<br>Literature (Ochs et al., 2006) and manufacturer information (Argex, 2012) |
| | Saturated hydraulic conductivity ($m\,s^{-1}$) | **$3.32 \times 10^{-3}$**<br>**$1 \times 10^{-2}$** | Bouzouidja (2012)<br>Technical specification (Leca®, 2012) |
| | Matrix potential at saturation (m) | **–0.010**<br>**–0.121**<br>**–0.405** | Value for organic matter (Lawrence and Slater, 2008)<br>Value for sand in ISBA (CH 1978[a])<br>Value for clay in ISBA (CH 1978[a]) |
| | *b*-coefficient for water retention curve (–) | **2.7**<br>**4.05**<br>**11.4** | Value for organic matter (Lawrence and Slater 2008)<br>Value for sand in ISBA (CH 1978[a])<br>Value for clay in ISBA (CH 1978[a]) |

[a] Clapp and Hornberger (1978).

**Table 5.** Statistical scores of GR water content, daily drainage and temperatures for the four best hydrological calibrations.

| Cal | Hydrological characteristics | | | | | Scores[a] | | | | | | | | | | | |
|---|---|---|---|---|---|---|---|---|---|---|---|---|---|---|---|---|---|
| | | | | | | Substrate water content | | | Outlet drainage | | | Substrate temperature | | | Drain. layer temperature | | |
| | | $W_{sat}$ | $k_{sat}$ | $\Psi_{sat}$ | $b$ | $R$ | NSE | BIAS | $R$ | NSE | BIAS | $R$ | NSE | BIAS | $R$ | NSE | BIAS |
| A | SUBS | 0.674 | $1.073 \times 10^{-3}$ | −0.100 | 3.9 | 0.73 | 0.018 | 1.3 | 0.52 | 0.022 | 119.3 | 0.93 | 0.613 | 2.09 | 0.91 | 0.645 | 0.55 |
| | DRAIN | 0.900 | $3.320 \times 10^{-3}$ | −0.010 | 2.7 | | | | | | | | | | | | |
| B | SUBS | 0.674 | $2.162 \times 10^{-3}$ | −0.100 | 3.9 | 0.73 | 0.019 | 1.3 | 0.52 | 0.023 | 119.2 | 0.93 | 0.613 | 2.09 | 0.91 | 0.645 | 0.55 |
| | DRAIN | 0.900 | $3.320 \times 10^{-3}$ | −0.010 | 2.7 | | | | | | | | | | | | |
| C | SUBS | 0.674 | $1.073 \times 10^{-3}$ | −0.932 | 3.9 | 0.72 | 0.064 | −3.3 | 0.56 | 0.081 | 129.7 | 0.93 | 0.601 | 2.12 | 0.91 | 0.636 | 0.57 |
| | DRAIN | 0.900 | $3.320 \times 10^{-3}$ | −0.121 | 2.7 | | | | | | | | | | | | |
| D | SUBS | 0.674 | $2.162 \times 10^{-3}$ | −0.932 | 3.9 | 0.72 | 0.064 | −3.3 | 0.56 | 0.082 | 129.7 | 0.93 | 0.601 | 2.12 | 0.91 | 0.636 | 0.57 |
| | DRAIN | 0.900 | $3.320 \times 10^{-3}$ | −0.121 | 2.7 | | | | | | | | | | | | |

[a] $R$ the coefficient of correlation (–), NSE the Nash-Sutcliffe Efficiency (–), BIAS the bias Model-Obs (in % for water content and drainage, in °C for temperatures).





GMDD
6, 1127–1172, 2013

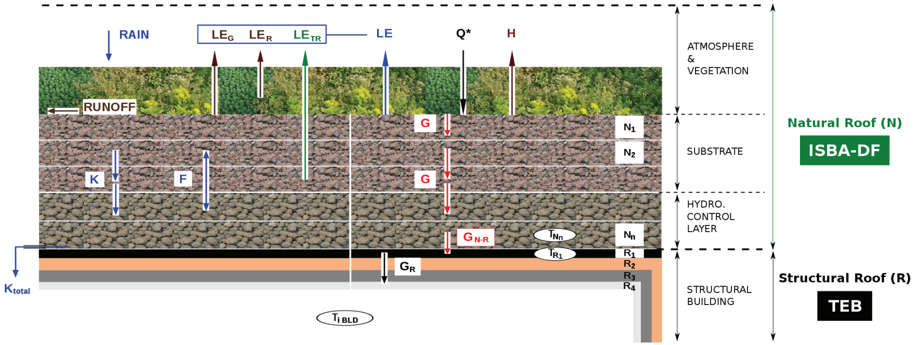


**Fig. 1.** Green roof design for TEB-GREENROOF and associated physical processes. Left: hydrological processes: surface run-off (RUNOFF), vertical water fluxes ($F$, infiltration or upward capillary action depending on moisture gradient), supersaturated drainage ($K$) and water drained out of the green roof base water ($K_{\text{total}}$) and precipitations (RAIN). Right: energy balance terms: net radiation ($Q^*$), sensible heat flux ($H$), latent heat flux ($LE$) and ground storage heat flux ($G$). $LE$ is the sum of the ground evaporation ($LE_{\text{G}}$), the evaporation of the water intercepted by the plant canopy ($LE_{\text{R}}$), and the vegetation transpiration ($LE_{\text{TR}}$). Right: thermal processes: within all layers, thermal conduction ($G$) between natural layers, $G_{\text{R}}$ between artificial layers, with $Q_{N-R}$ the heat flux coupling the natural and structural roofs.

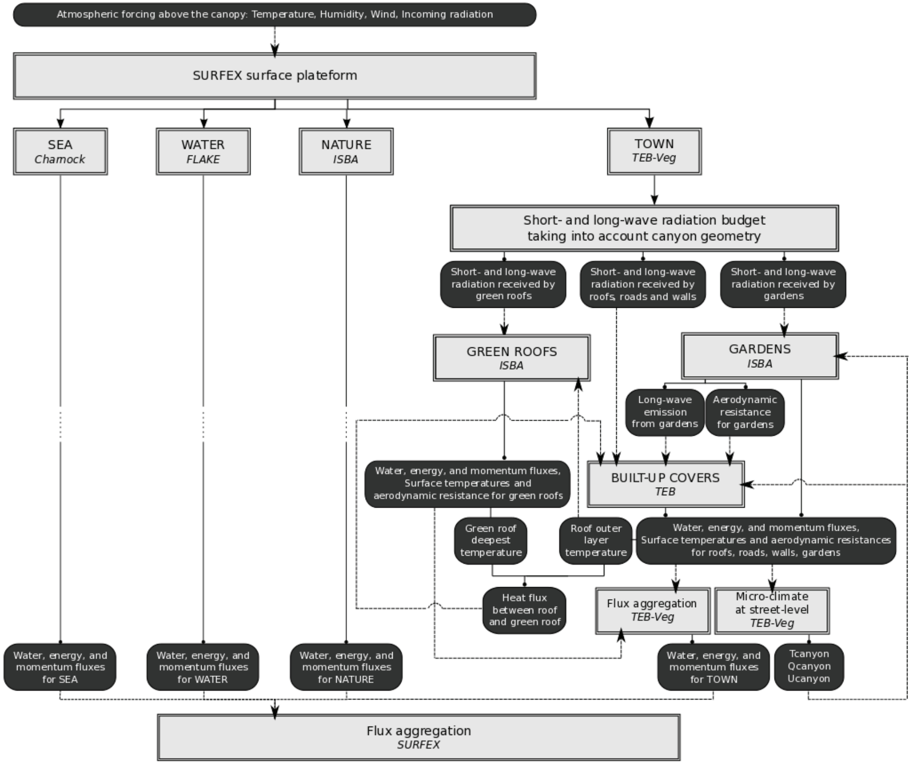


**Fig. 2.** Source code organisation of GREENROOF within TEB-Veg and SURFEX.





GMDD
6, 1127–1172, 2013

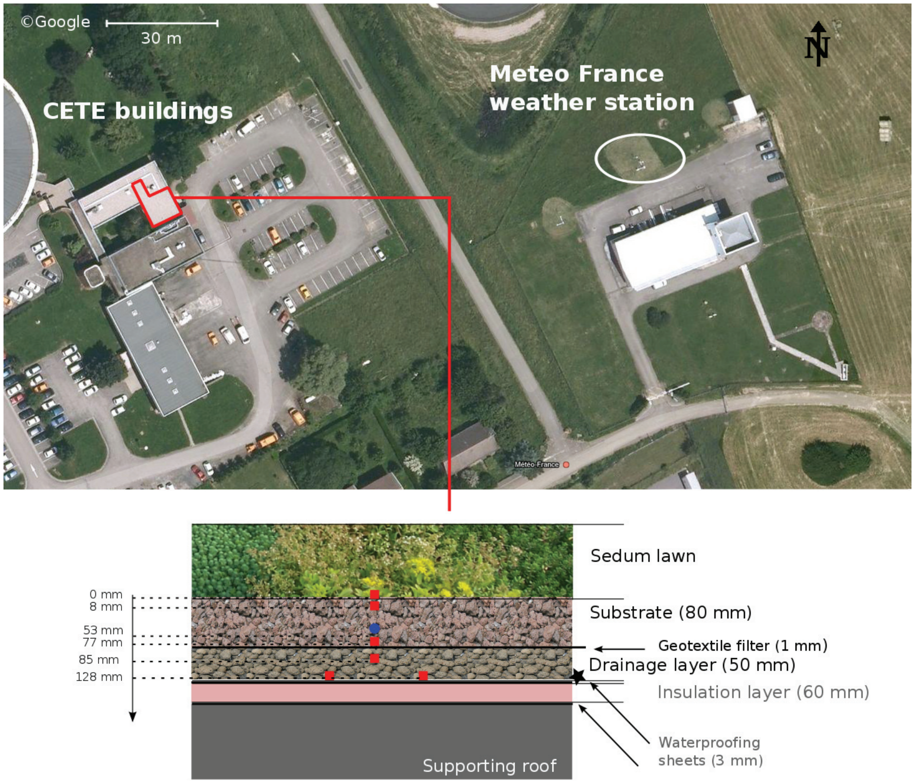


**Fig. 3.** Location (top) and design (bottom) of the green roof experimental plot modelled, showing the positions of sensors (squares for temperatures, circle for water content and matrix potential) and water outlet (star).





GMDD
6, 1127–1172, 2013

The GREENROOF module (v7.3) for TEB

C. S. de Munck et al.

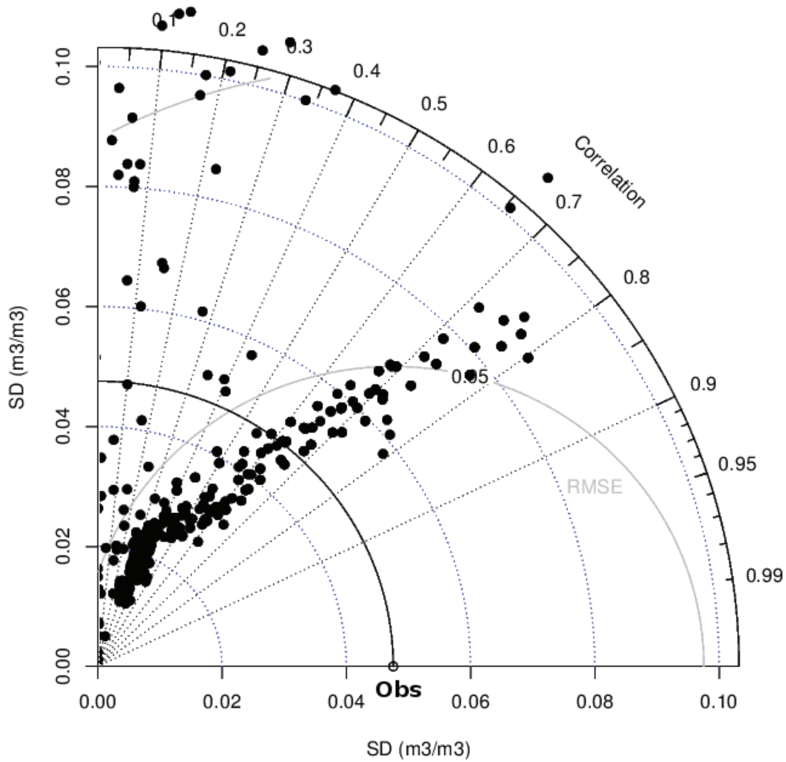


**Fig. 4.** Taylor diagram showing the performance of 576 models (differing in their hydrological characteristics) to model the water content recorded at 77 mm deep in the substrate of the GR plot studied. A dot is assigned to each of the 576 hydrologically calibrated simulations. One can read $R$ on the right hand side quadrant, SD radially ($SD_{OBS}$ is materialised by a black quadrant at $0.048\,m^3\,m^{-3}$), and the RMSE on grey semi-circles centered on the observations SD. The ideal model that would fit the observations is represented by the white dot ($R = 1$, $RMSE = 0$, $SD = SD_{OBS}$).





GMDD
6, 1127–1172, 2013
The GREENROOF module (v7.3) for TEB
C. S. de Munck et al.

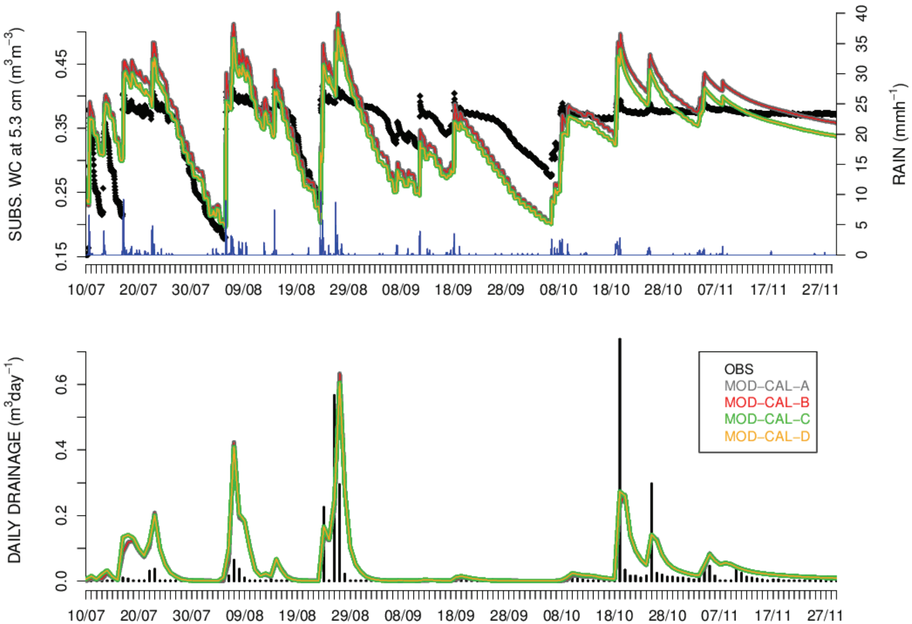


**Fig. 5.** Evolution between 4 July and 29 November 2011 of substrate water content (top) and daily outlet drainage (bottom), as observed and simulated by GREENROOF (with the four best hydrological calibrations).

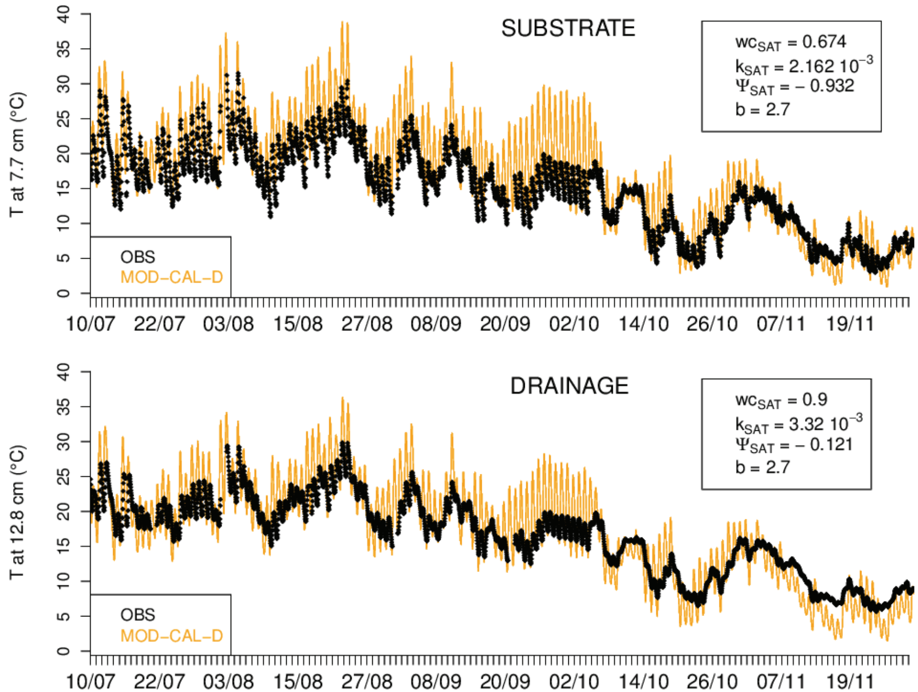


**Fig. 6.** Evolution between 4 July and 29 November 2011 of SUBSTRATE (top) and DRAINAGE layer (bottom) temperatures, as observed and simulated by GREENROOF (with the optimal hydrological calibration – characteristics presented in boxes, respectively for the SUBSTRATE (top) and DRAINAGE (bottom) layers).





GMDD
6, 1127–1172, 2013

The GREENROOF module (v7.3) for TEB

C. S. de Munck et al.

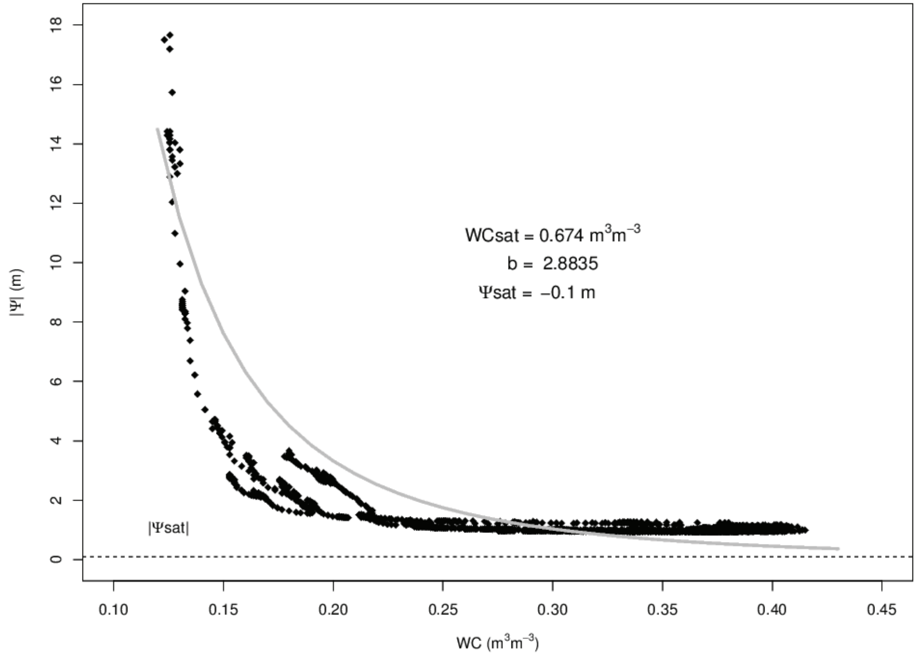


**Fig. A1.** Fitting water retention curve coefficient and matrix potential at saturation to observations when porosity = 0.411 $m^3 m^{-3}$.





GMDD
6, 1127–1172, 2013

The GREENROOF module (v7.3) for TEB

C. S. de Munck et al.

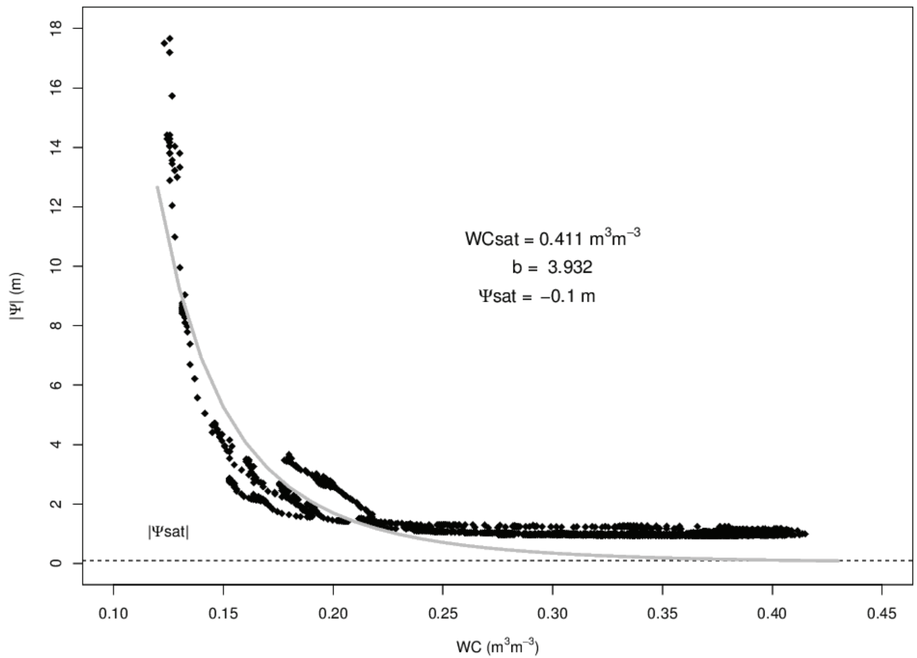


**Fig. A2.** Fitting water retention curve coefficient and matrix potential at saturation to observations when porosity = 0.674 $m^3\,m^{-3}$.